A Crude Introduction to Mott Insulators

J.C. de Boer - University of Twente

March 4th, 2015

Preface

This report is written as a way of noting my findings during a literature study on Mott insulators. Over the course of the past 8 months, I have been completing relevant courses, studied review articles and looked into related research that is going on at Twente University right now.

The intention of the performed study was to gain further insight in a specific correlated electron effect. The choice for Mott insulators was driven by the fact that the Mott metal-insulator transition is quite poorly covered in the solid state courses, despite it being a fairly common (and very interesting) effect. Furthermore, it is not easy to find an accessible but comprehensive text on Mott insulators, which makes this assignment more challenging. This report is supposed to bridge the gap between the egg crate models and the more sophisticated variations on the Hubbard model and describe the link with various analogous systems.

Index

1 Introduction

1.1 An introduction to correlated electrons

In the study of electrons in metals, the usual approach is to approximate the electronic system as a free electron gas (free electron model). Although somewhat rigorous, for most practical purposes, this approximation works reasonably well.

Common adjustments that make this model more realistic are those that consider a weak background potential due to the surrounding lattice (nearly free electron model) or a strong potential that binds electrons close to the nucleus (tight binding model). The background potential of the former model causes the formation of bands (the band theory of solids). Using Hartree-Fock we can even explain ferromagnetism in materials.

If we were to study a semiconductor, we would then define a small forbidden band with states that electrons can't occupy. If enough energy is supplied to the semiconductor and the gap is small enough, electrons become able to jump over this forbidden band gap and land in the conduction layer. This way we also have a toy model for semiconductors.

Upon further consideration, more interactions within the electronic structures can be thought of. Usually, most of these effects are negligible, but sometimes they dominate and can cause a metal-insulator transition.

1.2 The egg crate model

The widely adopted distinction between metals and insulators at 0 K is that metals have a partially filled highest band (Fermi level inside the conduction band) while insulators have a completely filled highest band (Fermi level inside forbidden band). Again, if the forbidden band is small enough, the insulator is called a semiconductor.

I would like to emphasize that in the rest of this report I will solely consider systems with temperatures so close to zero, that the probability of finding the system in an excited state due to thermal energy becomes very small. In other words, apart from the occasional induced excitation, the systems will be in their ground state.

In 1937, de Boer and Verwey [1] reported poor zero-temperature conduction in transition-metal oxides with partially filled d-bands. These materials were previously believed to be metallic, but they seemed to show insulating behaviour. Peierls and Mott (1937)[2] came up with the first possible explanation for this anomalous effect.

Mott then continued investigating the metal-insulator transition and took important steps towards a definite description of the special insulating state. This state became known as the Mott insulator and Mott attributed it to strong electron-electron interactions. If the d-band (just an energy band, no physical position) electrons are present on almost every site of the lattice, they repel an excited d-band electron so that it has no place to land for a long time. You can imagine that this long time without an atom to land on takes a large amount of energy that isn't present at very low temperatures. So therefore, if all other landing sites are occupied, electrons tend to stay in place.

A populair way of visualizing such a system, is by imagining egg-crates as the potential landscape caused by the periodic lattice and fill the egg crate with little balls (or eggs) that represent electrons. Figure 1 shows two egg crates; the one on the left with all sites occupied and the rightmost crate half-filled. If I were to tilt the egg crates so that the eggs tend to tumble down to a neighboring hole (applying a voltage to a sample is essentially a way of tilting the energy landscape), you intuitively "see" that the right crate is more susceptible to movement of the eggs.

Figure 1: Colorful egg crates; one filled and one half-filled.

2 Mathematical Frameworks

2.1 The classical approach

A simple mathematical model for the Mott insulating state can be obtained by comparing a few characteristic lengths and the electron concentration as in Gantmahker's Electrons and Disorder in Solids textbook [3]. Suppose we have an atomic lattice and a few ionized donor atoms that provide free, conducting electrons. The distance between these ionized donors is $a = n^{-1/3}$ (with n the ionized donor concentration) and the wavefunctions of these electrons falls of with increasing r as

$$\psi \propto \frac{e^{-r/a_0}}{r}, \tag{1}$$

where the Bohr radius $a_0 = 4\pi\epsilon_0\hbar^2 / m_e e^2$. The distance it takes to screen the potential of a charge carrier in a dilute electron gas is given by the Thomas-Fermi screening wave vector k_0. We can then define a screening radius

$$r_e = \frac{1}{k_0} = \sqrt{\frac{\pi\epsilon_0\hbar^2}{m_e e^2 n^{1/3}}}\ . \tag{2}$$

We can use the lengths a_0 and r_e to classify the electronic properties of the system. If $\boldsymbol{a_0 < r_e}$, all electrons remain within the radius where it is bound by the hosting atom, which corresponds to an **insulator**. However, if $\boldsymbol{a_0 > r_e}$, an electron may travel outside the screening radius where it no longer feels its atom and becomes delocalized, corresponding to **metallic** behaviour. If we now try to write r_e in terms of a_0 we get

$$r_e = \sqrt{\frac{\pi\epsilon_0\hbar^2}{m_e e^2 n^{1/3}}} = \sqrt{\frac{1}{4\,n^{1/3}}}\ \sqrt{\frac{4\pi\epsilon_0\hbar^2}{m_e e^2}} = \frac{1}{2}\sqrt{n^{-1/3}\,a_0}\ . \tag{3}$$

We can use this to determine the ionized donor concentration at which the system undergoes a metal-insulator transition by equating $r_e = a_0$:

$$r_e = \frac{1}{2}\sqrt{n^{-1/3}\,a_0} = a_0 \qquad \rightarrow \qquad n = \left(\frac{1}{4\,a_0}\right)^3. \tag{4}$$

This tells us that for $n > 0.25\,{a_0}^{-3}$ the system is in its metallic state. This condition has been experimentally verified for systems for which Eqs. 1 and 2 hold. Note that since the Mott MIT occurs at zero temperature and is induced by a tradeoff between parameters that determine the ground state energy of the system, the Mott metal-insulator transition is a quantum phase transition. This classical model however, is rather specific and not very quantum mechanical. In the next section we will look into a more sophisticated model.

2.2 The quantum mechanical approach

2.2.1 An intermezzo on notation

I do expect the reader to have some quantum mechanical background, but since I'll be using some second quantization notation which is not part of the standard master Applied Physics curriculum, I decided to include this intermezzo.

When you start with your first quantum mechanics course, you start using position representation to define wavefunctions of the form

$$\psi_k(\boldsymbol{r}) = A\,e^{i\boldsymbol{k}\cdot\boldsymbol{r}} \tag{5}$$

which describes the particle's position and energy (via wave vector $\boldsymbol{k}$).

Now consider an electron that can be located at 3 different sites and can have 2 different values for $\boldsymbol{k}$, which amounts to 6 possible states in total. If we define a list of single electron states in the form $|\boldsymbol{r}_1, \boldsymbol{k}_1; \boldsymbol{r}_1, \boldsymbol{k}_2; \boldsymbol{r}_2, \boldsymbol{k}_1; \boldsymbol{r}_2, \boldsymbol{k}_2; \boldsymbol{r}_3, \boldsymbol{k}_1; \boldsymbol{r}_3, \boldsymbol{k}_2\rangle$ and hold on to this order of states, we can write the state of a system with an electron at site $\boldsymbol{r}_2$ and with $\boldsymbol{k}$ -vector $\boldsymbol{k}_1$ as $|0;\ 0;\ 1;\ 0;\ 0;\ 0\rangle$. In this notation, the state of the system is described by a list of the numbers of electrons per single electron state. This "second quantization" notation is also called "number representation" for obvious reasons.

As you may have figured, $|0;\ 0;\ 0;\ 0;\ 0;\ 0\rangle$ would describe the vacuum state of the system. The operator $\hat{c}^{\dagger}_{r_3\,k_1}$ is a "creation operator" that creates an electron at position $\boldsymbol{r}_3$ and with $\boldsymbol{k}$ -vector $\boldsymbol{k}_1$. In action, the operator looks like this:

$$\hat{c}^{\dagger}_{r_3\,k_1}\,|0,\ 0,\ 0,\ 0,\ 0,\ 0\rangle = |0,\ 0,\ 0,\ 0,\ 1,\ 0\rangle. \tag{6}$$

Similarly,

$$\hat{c}^{\dagger}_{r_1\,k_2}\,\hat{c}^{\dagger}_{r_3\,k_1}\,|0,\ 0,\ 0,\ 0,\ 0,\ 0\rangle = |0,\ 1,\ 0,\ 0,\ 1,\ 0\rangle, \tag{7}$$

which shows us that we can build any state of the system (itself a combination of single electron states) out of the ground state $|\ 0\ ,\ 0\ ,\ 0\ ,\ 0\ ,\ 0\ ,\ 0\ \rangle$.

The counterpart of $\hat{c}^{\dagger}_{r_3\,k_1}$ is $\hat{c}_{r_3\,k_1}$, which "annihilates" or "destroys" an electron in the specified state and is appropriately called an "annihilation operator". We can use it to reverse Eq. 7 for example:

$$\hat{c}_{r_3\,k_1}\,\hat{c}_{r_1\,k_2}\,|0,\ 1,\ 0,\ 0,\ 1,\ 0\rangle = |0,\ 0,\ 0,\ 0,\ 0,\ 0\rangle. \tag{8}$$

If the operators result in a state that doesn't exist, such as a state with 2 spin up electrons at the same position or a system with -1 electrons in a certain state, the operation results in a 0. Notice that

$$\hat{c}^{\dagger}_{r_3\,k_1}\,\hat{c}_{r_3\,k_1}\,|0,\ 0,\ 0,\ 0,\ 1,\ 0\rangle = 1 \quad \text{and} \quad \hat{c}^{\dagger}_{r_3\,k_1}\,\hat{c}_{r_3\,k_1}\,|0,\ 0,\ 0,\ 0,\ 0,\ 0\rangle = 0 \tag{9}$$

result in the number of electrons in state $\boldsymbol{r}_3\,\boldsymbol{k}_1$. We define the number operator $\hat{n}_{\boldsymbol{r}_3\,\boldsymbol{k}_1} = \hat{c}^{\dagger}_{\boldsymbol{r}_3\,\boldsymbol{k}_1}\,\hat{c}_{\boldsymbol{r}_3\,\boldsymbol{k}_1}$, which counts the number of electrons in the specified state. We now have introduced enough operators to describe the Hubbard Hamiltonian in second quantization language.

2.2.2 The bare Hubbard model

In 1963, John Hubbard came up with his famous Hubbard model [4]. It describes a Hamiltonian that combines a "hopping term" with a term that describes the on-site electron-electron repulsion. The former originates from the tight binding model. The tight binding model's most important feature is the inter-site element that describes the hopping of electrons from one site to another. The hopping parameter $t(\boldsymbol{R})$ for hopping from site $\boldsymbol{r}$ to a site at position $\boldsymbol{R}$ is defined as

$$t(\boldsymbol{R}) = \int \phi^{*}(\boldsymbol{r})\ U(\boldsymbol{r})\,\phi(\boldsymbol{r}-\boldsymbol{R})\,d^3\,r \tag{10}$$

i.e. the effect of the atomic potential at $\boldsymbol{r}$ on the overlap integral between different sites. Hubbard uses this parameter to define his hopping term in second quantization language:

$$\mathcal{H}_t = -\,t_{i,j} \sum_{\text{all } i,\,j,\,\sigma\,;\,i\neq j} \left(\hat{c}^{\dagger}_{i,\sigma}\,\hat{c}_{j,\sigma} + \hat{c}^{\dagger}_{j,\sigma}\,\hat{c}_{i,\sigma}\right). \tag{11}$$

It describes all possible ways for an electron of spin σ to be annihilated at site j and created at site i, or vice versa. The minus sign in front of the t is because this term usually lowers the energy. The on-site electron-electron repulsion term (or potential term) is written as

$$\mathcal{H}_U = U \sum_{\text{all } i} \hat{c}^{\dagger}_{i\uparrow}\,\hat{c}_{i\uparrow}\,\hat{c}^{\dagger}_{i\downarrow}\,\hat{c}_{i\downarrow} = U \sum_{\text{all } i} \hat{n}_{i\uparrow}\,\hat{n}_{i\downarrow}. \tag{12}$$

This term adds a U (Coulomb repulsion) to the total energy for every doubly occupied site, i.e. contains both a spin up and a spin down electron. It reflects the additional energy required to force 2 negatively charged electrons into the same site.

Frequently, an extra term is added to the Hamiltonian for controlling the fill fraction. With μ the chemical potential, this term has the form

$$-\mu \sum_{\text{all } i} (\hat{n}_{i\uparrow} + \hat{n}_{i\downarrow}). \tag{13}$$

If we were dealing with bosons, the ground state of the system would have all particles in the same state. But since the electric Mott insulator is a fermionic electron system, Pauli's exclusion principle allows only 2 particles of opposite spin per site of our system. Because we are usually interested in half-filled systems (one electron on each site instead of 2 of different spin), the chemical potential is often shifted by $U/2$ so that the total Hubbard Hamiltonian becomes:

$$\mathcal{H}_H = -t_{i,j} \sum_{i,\,j,\,\sigma\,;\,i\neq j} \left(\hat{c}^{\dagger}_{i,\sigma}\,\hat{c}_{j,\sigma} + \hat{c}^{\dagger}_{j,\sigma}\,\hat{c}_{i,\sigma}\right) + U \sum_{i} \left(\hat{n}_{i\uparrow} - \frac{1}{2}\right)\left(\hat{n}_{i\downarrow} - \frac{1}{2}\right). \tag{14}$$

Or simply

$$\mathcal{H}_H = \mathcal{H}_t + \mathcal{H}_U - \mu\, N, \tag{15}$$

where $N = \sum_i (\hat{n}_{i\uparrow} + \hat{n}_{i\downarrow})$. Hubbard's Hamiltonian shows that the energy of the system is a tradeoff between the energy gained by the hopping itself and the energy lost by putting 2 electrons on one site. Figure 2 shows a diagram that shows how the ratio hopping-repulsion varies with the fill fraction. Clearly visible is how around half integer filling, the potential term is most dominant. If however, the hopping term is large enough (or the potential term small enough) the system is very metallic. Diagrams of this t/U form are extensively used to describe Mott metal-insulator transitions.

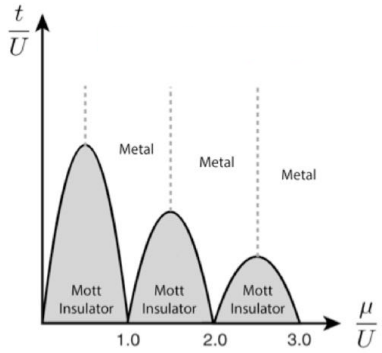

Figure 3: t/U diagram with critical points at half-integer fill fractions. (by Fischer et al, PRB, 1989)

2.2.3 Extensions to the Hubbard model

The Hubbard model we discussed in the previous section, has quite a few shortcomings. Here, we will look into these and discuss some extensions to the Hubbard model that make for a better approximation.

One quite crude simplification is that the Hubbard model only considers a single band. Many transition metal based materials however, have (partially) filled $3d$ bands and may have $4s$ and $4p$ bands at similar energies. Lattice symmetries often cause the $3d$ band to split in separate e_g and $t_{2\,g}$ bands, which may in turn split into $d_{x^2-y^2}$, $d_{3\,z^2-r^2}$ and $d_{x\,y}$, $d_{y\,z}$, $d_{z\,x}$ orbitals respectively. Now we have a lot of orbitals to consider and all the corresponding hybridization effects.

Let's assume that we are lucky and have a system where the $4s$ and $4p$ bands are far away from the $3d$ band and there is no hybridization between the p and $3d$ bands into a single effective single band. Furthermore, the splitting within the e_g and t_{2g} bands is weak so that we have 2 degenerate orbitals for e_g and 3 for t_{2g}. For this problem there is a modified Hubbard model called the degenerate Hubbard model that deals with all bands ν:

$$\mathcal{H}_{DH} = \mathcal{H}_{Dt} + \mathcal{H}_{DU} + \mathcal{H}_{DUJ}. \tag{16}$$

Here we write the first two terms as

$$\mathcal{H}_{Dt} = -\sum_{\langle i,j\rangle,\sigma,\nu,\nu'} t_{i,j}^{\nu,\nu'} \left(\hat{c}_{i,\sigma,\nu}^{\dagger}\,\hat{c}_{j,\sigma,\nu'} + \hat{c}_{j,\sigma,\nu}^{\dagger}\,\hat{c}_{i,\sigma,\nu'}\right) \tag{17}$$

$$\mathcal{H}_{DU} = \sum_{i,\sigma,\sigma',\nu,\nu'} \left(1-\delta_{\nu,\nu'}\,\delta_{\sigma,\sigma'}\right) U_{\nu,\nu'}\,\hat{n}_{i,\sigma,\nu}\,\hat{n}_{i,\sigma',\nu'} \tag{18}$$

where we added hopping from one band on site i to another band on site j to the hopping term and slightly altered notation in the potential term. $\mathcal{H}_{DU}$ now includes the Pauli exclusion principle with a factor $\left(1-\delta_{\nu,\nu'}\,\delta_{\sigma,\sigma'}\right)$ and covers all intrasite Coulomb interactions, whatever band the electrons may be in (inter-orbital Coulomb interaction).

The $\mathcal{H}_{DUJ}$ term is the "intrasite exchange interaction" which looks as complicated as it sounds:

$$\mathcal{H}_{DUJ} = -\sum_{i,\sigma,\sigma',\nu,\nu'} J_{\nu,\nu'}\Big[\left(1-\delta_{\nu,\nu'}\right)\hat{c}_{i,\sigma,\nu}^{\dagger}\,\hat{c}_{i,\sigma',\nu}\,\hat{c}_{i,\sigma',\nu'}^{\dagger}\,\hat{c}_{i,\sigma,\nu'} - \left(1-\delta_{\nu\nu'}\right)\left(1-\delta_{\sigma\sigma'}\right)\hat{c}_{i,\sigma',\nu'}^{\dagger}\,\hat{c}_{i,\sigma,\nu}^{\dagger}\,\hat{c}_{i,\sigma,\nu}\,\hat{c}_{i,\sigma',\nu}\Big]. \tag{19}$$

The first term lowers the system's energy if spins on different orbitals (but on the same site of course) have aligned spin. For the quantum mechanically educated amongst you, Hund's first rule may now come to mind and that is exactly what Eq.19 represents. $J_{\nu,\nu'}$ is a factor defined by

$$J_{\nu,\nu'} = \int \phi_i^{\nu}(\boldsymbol{r})\,\phi_i^{\nu'}(\boldsymbol{r})\,\frac{e^2}{|\boldsymbol{r}-\boldsymbol{r}'|}\,\phi_i^{\nu}(\boldsymbol{r}')\,\phi_i^{\nu'}(\boldsymbol{r}')\,d^3\boldsymbol{r}. \tag{20}$$

You may also choose to incorporate an intersite exchange term, but this quickly becomes very complicated due to anisotropy in exchange coupling. For a more detailed discussion on an exchange Hamiltonian in the strong coupling limit, I refer you to Eq. 2.8 of a great review article by Imada et al. (1998) [5].

Now that we have incorporated multiple bands in our model, we look further for simplifications in the Hubbard model and find that we could improve it by including more than only the on-site Coulomb repulsion. To do so, we can introduce a $\mathcal{H}_{DV}$ term to incorporate the nearest neighbour Coulomb interactions:

$$\mathcal{H}_{DV} = \sum_{\langle i,j\rangle,\sigma,\sigma',\nu,\nu'} V_{i,j}^{\nu,\nu'}\,\hat{n}_{i,\sigma,\nu}\,\hat{n}_{j,\sigma',\nu'}. \tag{21}$$

It just adds the matrix element $V_{i,j}^{\nu,\nu'}$ for every nearest neigbour electron it finds, whatever its spin or orbital is. We now have

$$\mathcal{H}_{DH} = \mathcal{H}_{Dt} + \mathcal{H}_{DU} + \mathcal{H}_{DUJ} + \mathcal{H}_{DV}, \tag{22}$$

which has become quite a feisty equation if you write out all the terms. In the following chapters, we will come across even more derivations from the Hubbard model.

3 Optical Trap Mott Insulators

3.1 An introduction to optical Mott systems

There are artificial ways to model Mott insulators. One such way is to trap atoms in an "optical lattice". One advantage of optical lattices is that they can be constructed in 1, 2 and 3D forms. These lattices are build from lasers with nodes at the lattice points. In 1D the setup is rather straightforward and gives a pattern as in the left of Figure 4. For 2D lattices, the setup is a little more complicated and allows for more different structures. For us, the most relevant lattice is the square lattice as shown in the right of Figure 4. If one uses 6 lasers in a configuration as in the left of Figure 5 (where the small arrows indicate the polarisation of the light), one obtains a 3D square lattice as on the right hand side of the same figure.

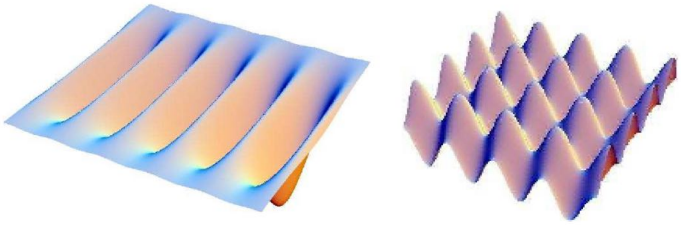

Figure 4: 1 and 2D Optical lattices (van Oosten, 2004 [6]).

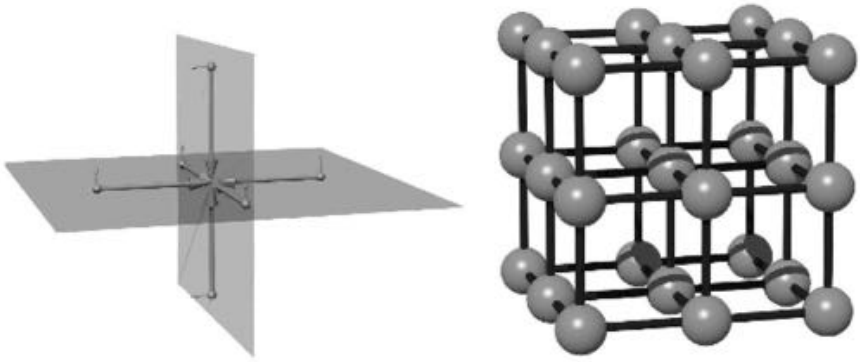

Figure 5: 3D Optical square lattice and the corresponding laser setup (van Oosten, 2004 [6]).

The conventional method of trapping atoms in an optical trap, was to first trap several atoms in a magneto optical trap (MOT) and then catch these in the optical lattice. However, the atom density would be very low as a MOT traps $\sim 10^{10}$ atoms per cm^3 and the density of the lattice sites is $(\lambda/2)^{-3} \sim 10^{14}$ per cm^3. This is not enough to model a Mott insulator as we know by now.

Fortunately, we can also load the lattice with a Bose-Einstein condensate via a magnetic trap, which gives us several atoms per lattice site. Just like with electric Mott instulators and vortex Mott systems, we would have to use extremely low temperatures to experiment with optical Mott insulators. Optical cooling is not sufficient in this case because it fails at the required high densities. Instead, evaporative cooling is used in mentioned magnetic trap to reach Bose-Einstein condensates.

The Hamiltonian that governs the optical Mott insulator system is called the Bose-Hubbard Hamiltonian and is given by:

$$\mathcal{H}_{\mathrm{BH}} = -t_{i,j} \sum_{\langle i,j \rangle} \hat{a}_i^\dagger \, \hat{a}_j + \frac{1}{2} \, U \sum_i \hat{a}_i^\dagger \, \hat{a}_i^\dagger \, \hat{a}_i \, \hat{a}_i - \mu \, \hat{a}_i^\dagger \, \hat{a}_i. \tag{23}$$

The main differences with the fermionic Hubbard Hamiltonian are bosonic operators $\hat{a}_i^\dagger$ and $\hat{a}_i$, the absence of a spin constraint as the Pauli exclusion principle and the sign inversion upon exchange of position. Over the last decade, these kind of setups have been well studied, including similar optical systems with fermionic atom gasses.

3.2 Optical Mott insulators in practice

In september 2008, Jördans et. al. [7] published an article that describes how they prepared a quantum degenerate gas of fermionic ^{40}K atoms and used it in an optical lattice to simulate the fermionic Mott insulating system. Due to the simple cubic lattice, each atom feels $6t$ (denoted by Jördans et. al. as $6J$) attractive and U repulsive force. The lefthand plot in Figure x shows how tuning the $U/6t$ ratio affects the average occupation number of each site depending on the total number of atoms in the system. It clearly shows how switching the repulsive force on causes the atoms to form a Mott insulating system with very little double occupations. In the same article they also report observations of a gapped mode in the excitation spectrum of their fermionic optical Mott insulator. The rightmost plot of Figure 6 shows a distinct peak that marks the gap.

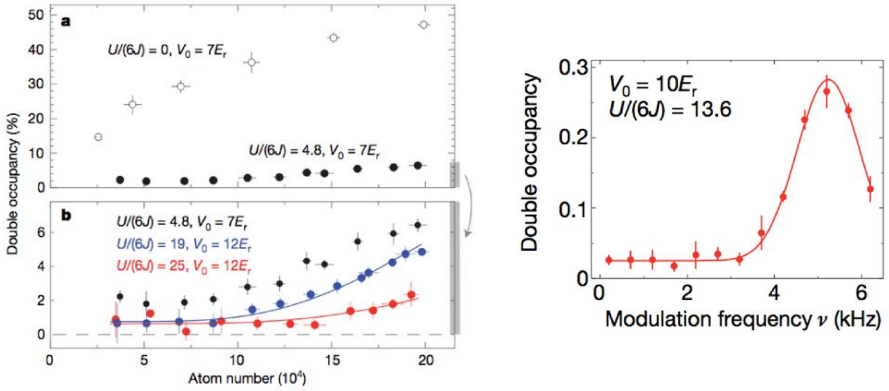

Figure 6: Left: Average occupation number as a function of total atom number and Right: A gapped mode in the excitation spectrum (Jördans et. al. 2008 [7]).

Another feature that really confirms the Mott insulating behavior is the incompressibility of the atom gasses near integer filling. The compressibility $\frac{\partial n}{\partial \mu}$ is observable as $\frac{\partial D}{\partial N}$ where D is the number of doubly occupied states and N is the total number of atoms in the system. The left image in Figure 7 shows the idea that instead of a smooth linear curve in the superfluid regime, a staircase would be apparent in the Mott regime. Vanishing of the compressibility was measured by Jördans et. al. 2008 near potential modulation of $U / h = 4\,\mathrm{kHz}$.

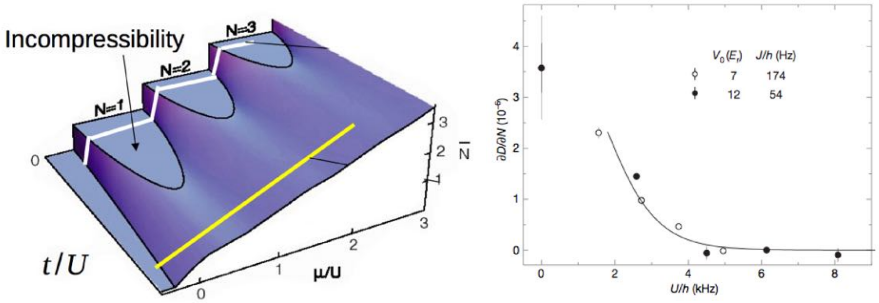

Figure 7: Incompressibility near Mott insulating regimes by Left: Dupius, N (2008) and Right: Jördans et. al. 2008.

3.3 A bosonic Mott model for visualisation

I attempted to make a simpel model that mimics bosonic Mott behaviour like in the optical systems of this chapter. Modeling this using realistic electron wavefunctions and Hubbard Hamiltonians requires computational techniques that are way beyond the scope of this report and is rather unnecessary as the model's mere purpose is to visualize a principle.

The model I wrote in mathematica simulates a 2D simple square lattice of 10x20 lattice spacings large, with a variable number of electrons and holes present. The only allowed electron movement is in the horizontal direction towards the right, which makes it effectively a row of 1D systems. I have chosen to completely ignore intersite potentials and simply let every electron look whether the site in front of it is free or not. Actually, as the problem is most interesting near 80-100% occupation of the lattice sites (only one vacancy per site), I have simulated hole hopping to make computations easier.

No boundary conditions were imposed on the upper and lower side of the lattice since only horizontal movement is allowed. The horizontal boundary condition is that every hole that hops off the left edge of the sheet, reincarnates on the right edge at the same y-coordinate so that you may think of the 2D sheet as a cylinder with circulating electrons and holes.

The result allows the user to select a fill fraction and observe how it affects the dynamics of the electrons (red) and holes (blue) as shown in Figure 8. The reason I wrote it in *Mathematica* is that it is supposedly easy to embed dynamic *Mathematica* content into webpages, but upon further examination, this proved to be not so straightforward. Instead, I added the script for the model in the appendix of this report so that it can be run in *Wolfram Mathematica* via copy-pasting.

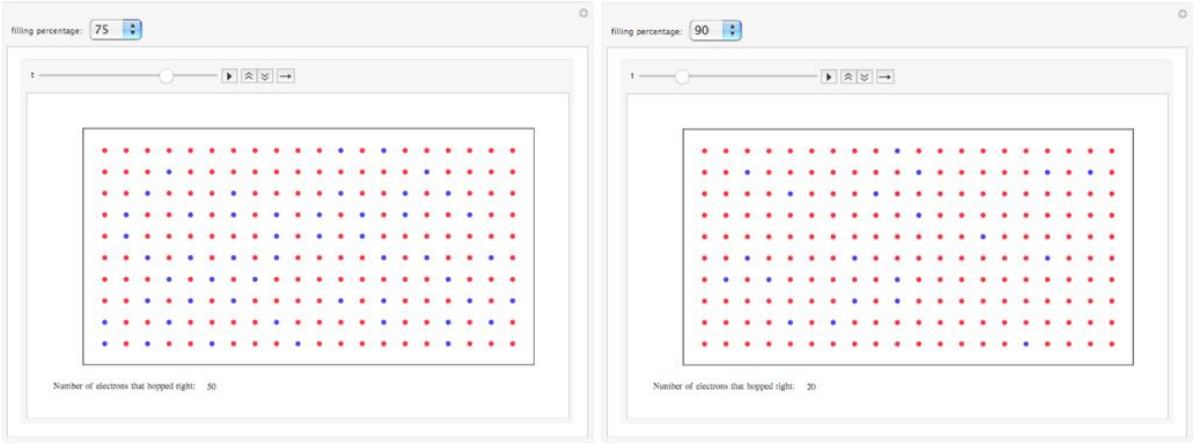

Figure 8: Interface that visualizes hopping holes and electrons (highly simplified model)

The physics here is highly simplified, but the model serves its job as a simple egg-crate toy model. At 100% filling (one electron on every site), the system is stuck and no single electron can hop until the force exerted on it is high enough to push it in the next energy level. Since only a single level exists in this overly simplified model, the model only simulates what happens between the critical points.

While toying around, I noticed that at 50% filling (100 electrons and 100 holes), the number of hopping holes or electrons per second converged to ~80. This is of course due to some rows that contain slightly more holes (or electrons) so that "traffic jams" occur, while I did not allow the holes to hop into a less occupied "lane". This problem is one of optimal conductivitiy depending on fill fraction and probably is not within the scope of this report. But it does illustrate the purpose of building Mott toy models as is often done with much more advanced techniques and especially, more correct physics.

4 Vortex Mott Insulator Systems

4.1 Vortex Mott; a short introduction

Aside from optical systems, more ways have been found to model Mott insulator behavior. In 1993, David R. Nelson and V.M. Vinokur [8] published a paper that describes a dynamic vortex system with 2D Mott insulator-like effects. The idea is to prepare an array of superconducting islands (Figure 9, left) so that an applied magnetic field causes vortices between the superconducting islands. Varying the magnetic field strength is the obvious way of controlling the vortex fill fraction while a current of vortices can be measured as flux flow resistivity. This vortex current is induced by a bias de-pinning current (Figure 8, right). Table 1 shows how the different properties of a vortex Mott system map to an electrical Mott insulator.

Table 1: Mapping of vortex Mott system on an electrical Mott insulator

	Electric Mott system	Vortex Mott System
Dynamic component	Electric current	Vortex flow
Fill fraction control	Dopants	Magnetic field strength
Cause of movement	Bias voltage	Bias de-pinning current
Detection of movement	Coulombs / sec	Differential flux flow resistivity
Cause of repulsion	Coulomb force	Lorentz force

Years later, Vinokur collaborated with the Interfaces and Correlated Electron systems (ICE) group at Twente University to continue research on these vortex Mott systems [9]. They used a 4-point Van der Pauw configuration gold layer on a substrate with a square lattice of superconducting niobium islands (spacing $a = 267\,\mathrm{nm}$) on top. The fill fraction of the vortex system is given by $f = B\,/\,B_0$, that is, the applied field divided by the field of a single flux; $B_0 = \frac{\pi\hbar}{e\,a^2} \sim 28.6\,\mathrm{mT}$. It seems reasonable to expect Mott insulator phases at all integer fill fractions as was shown in Figure 3. In fact, Mott insulating behaviour was measured at even more fill fractions.

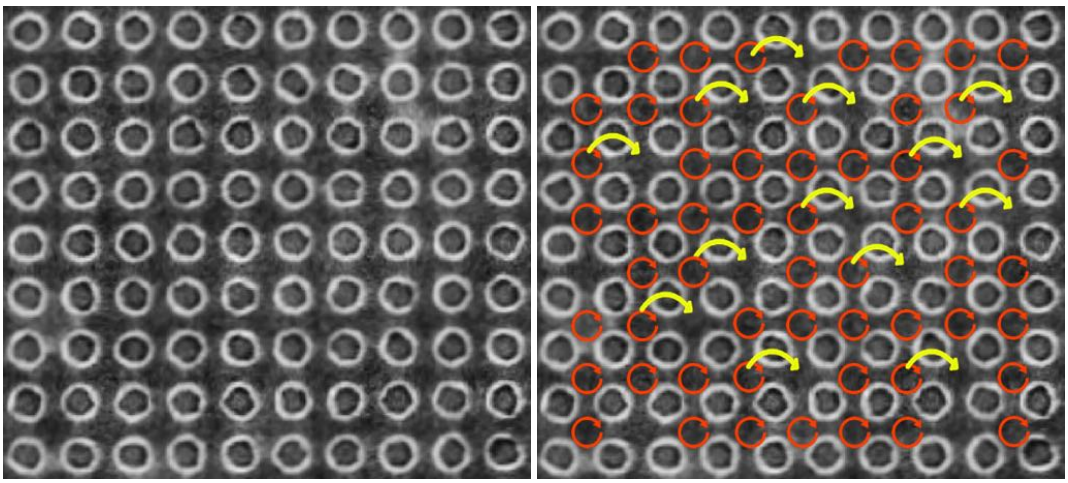

Figure 9: Left; Array of superconducting Nb islands on Au substrate. Right; Same array but with moving vortices. (Original SEM image by ICE group at Twente University (2014), modified by J.C. de Boer)

4.2 Interesting results of vortex Mott measurements

Because the vortex Mott insulating phase depends both on fill fraction and on bias current, the measurements were performed at several different bias currents and varying magnetic field. At $f = 1$ and $f = 2$, which correspond to full and double filling of the vortex array, Mott insulating phases were observed as points where the differential resistance dropped close to zero (see Figure 10). At a certain threshold breakdown current however, the hopping force becomes greater than the repelling force, so that a vortex current flows. In fact, maxima occur when the breakdown current is reached near integer filling. Possibly, these maxima occur because of the large amount of vacancies available at this point. This min-max flipping is quite pronounced and occurs even at fractional filling. Flips at integer and half integer fill fractions are indicated with arrows in Figure 9, but flipping is also apparent at $\frac{1}{3}$ and $\frac{2}{3}$ fill fractions, especially for the lower bias currents.

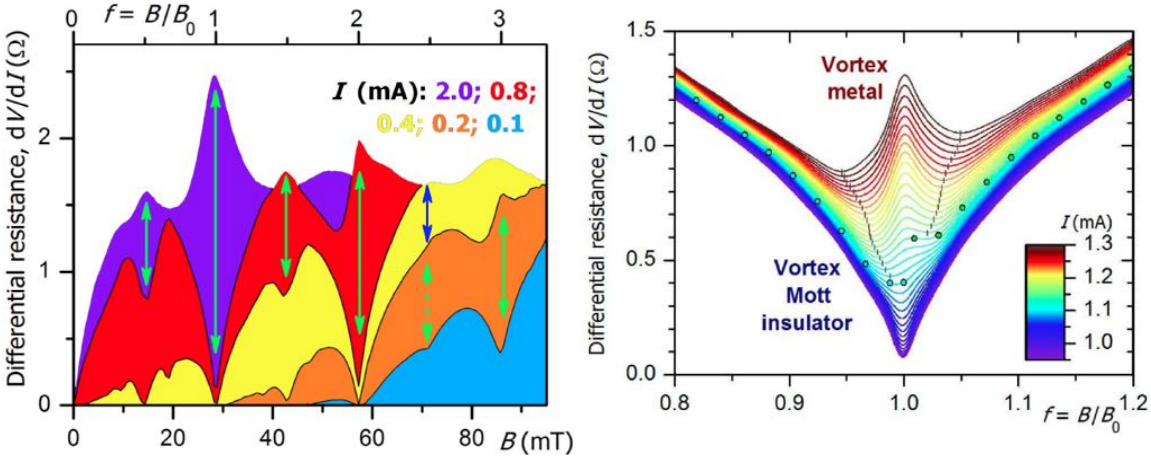

Figure 10: Plot of the differential resistance as a function of fill fraction. Higher differential resistance indicates more flux hopping. The arrows indicate flipping of minima to maxima at the Mott metal-insulator transitions. It may be a small detail, but in my opinion the dotted green arrow was wrong so I replaced it by the blue one. The right image shows the transition for different depinning currents. (Original by ICE group at Twente University (2014), modified by J.C. de Boer)

Upon solving the Harper equation (which I shall not further discuss in this report), energy minima have been found at $f = \frac{1}{3}, \frac{1}{2}, \frac{2}{3}, \frac{4}{3}, \frac{3}{2}, \frac{5}{3}$, ..., which reflects modulations of the ground state of the system as is visualized in Figure 11. It is tempting to propose a link between those effects at fractional filling and the fractional quantum hall effect. The validity of this connection has yet to be examined.

If one thinks of a vortex as a spin up and a vacancy as a spin down, one sees the similarity between the $f = \frac{1}{2}$ vortex Mott system and an antiferromagnet. We will come across this antiferromagnetic behaviour later.

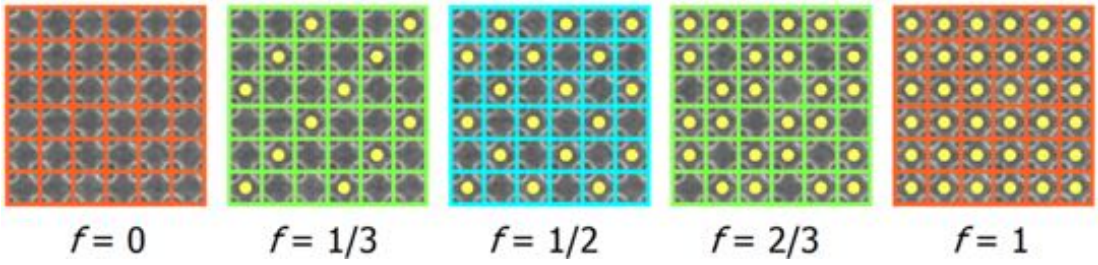

Figure 11: Modulated vortex patterns at fractional filling (by ICE group at Twente University, 2014).

4.3 Scaling in vortex-Mott systems

The ICE group explored the behaviour of Mott systems near the critical transition point through the theory of scaling. This theory aims to describe the quantum phase transition as a function of a single variable order parameter. Kotliar et. al. (2000) **[10]** used a mean field version of the Hubbard model to find that at constant temperature lines and centered about the critical fill fraction h, the width of U, ΔU scales as $(T_c - T)^{\delta/(\delta-1)}$, where δ follows from the scaling of the source field with the order parameter. Kotliar et. al. used a Weiss source field which gave them a $\Delta U \propto (T_c - T)^{3/2}$ dependency ($\delta = 3$).

The temperature and pressure driven Mott system maps to the vortex-Mott system as $|T - T_c| \rightarrow |I - I_c|$ and $|U - U_c| \rightarrow h = |f - f_c|$. The ICE group plotted their measurement results as $|I - I_c|$ vs $h = |f - f_c|$ and since it appeared that approaching critical filling from the left or right differed, both were analysed separately. The asymmetry may reflect electron and hole tunneling dynamics, just like critical temperatures of electron and hole doped Mott insulators do. The plots for the critical fillings $f = \frac{1}{2}$, 1 and 2 are given in Figure 11.

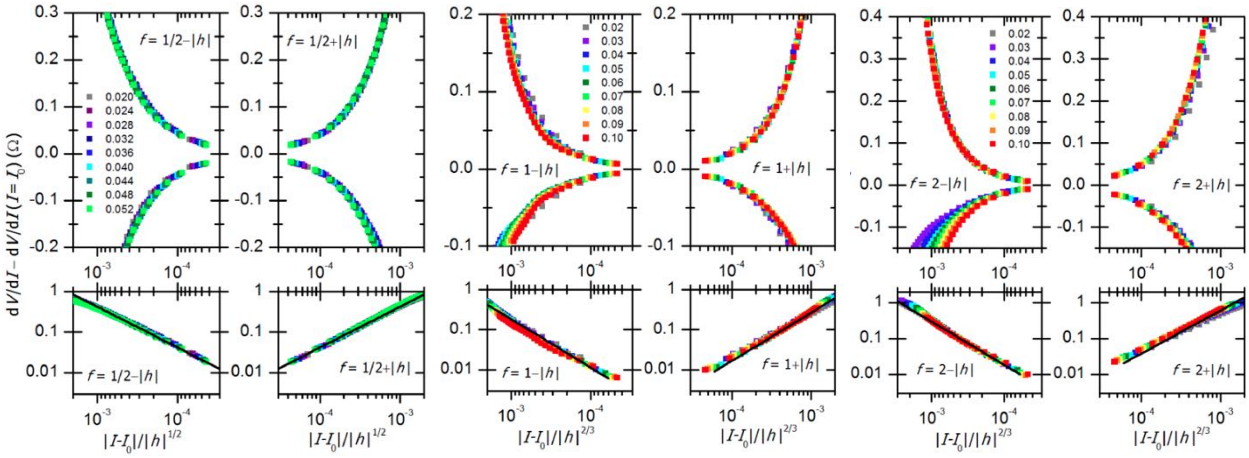

Figure 12: Dynamic behaviour of vortex-Mott system near critical point for $f = \frac{1}{2}$, 1, 2 (by ICE group at Twente University, 2014).

Upon fitting $(T_c - T)^{\delta/(\delta-1)}$ lines on the data presented in Figure 12, best fits were found for $\delta = 2$ for $f = \frac{1}{2}$ and $\delta = 3$ for $f = 1$ and 2. Notably, the optimal δ values were found to be identical for approaching the critical point from either left or right-hand sides, despite the apparent asymmetry in the right plot of Figure 10. In log-log form (lower panels of Figure 12) the data shows x^{μ} power law behaviour with $\mu = 1 \pm 0.03$ for $f = \frac{1}{2}$ and $\mu = 1.2 \pm 0.03$ for $f = 1$ and 2.

So not only does the vortex system exhibit Mott-like behaviour, it is also able to accurately validate theoretical models regarding the dynamic Mott transition by well defined vortex-particle mapping. Comparing it to optical Mott insulator systems, the vortex-Mott lacks the ability to introduce more complicating effects such as spin-orbit coupling and a 3D vortex system seems out of the question. The vortex-Mott does however seem easier to build and operate than an optical system.

5 Mott Insulators and Superconductivity

5.1 Antiferromagnetism

An interesting class of Mott insulators are the high-T_c cuprates with their CuO_x planes (Figure 12). The exchange interaction between the Cu d-orbitals occurs through the ligand p-orbitals on the oxygen atoms, which are hybridized with their neighbouring d-orbitals. This long range exchange mechanism is called "superexchange" and allows to be described by the Heisenberg Hamiltonian:

$$\mathcal{H}_{\text{Heis}} = J \sum_{\langle i,j \rangle} \boldsymbol{S}_i \cdot \boldsymbol{S}_j, \tag{24}$$

where $J = 4\,t^2 / U$ for systems that can be described by the Hubbard model. If we boldly add this to the hopping term and include a Coulomb term, we obtain Józef Spałek's [10] celebrated t-J model:

$$\mathcal{H}_{t-J} = -t_{i,j} \sum_{\text{all } i,\,j,\,\sigma\,;\,i \neq j} \left(\hat{c}^{\dagger}_{i,\sigma}\,\hat{c}_{j,\sigma} + \hat{c}^{\dagger}_{j,\sigma}\,\hat{c}_{i,\sigma}\right) + J \sum_{\langle i,j \rangle} \left(\boldsymbol{S}_i \cdot \boldsymbol{S}_j - \frac{1}{4}\,\hat{n}_i\,\hat{n}_j\right). \tag{25}$$

The superexchange in these cuprates causes them to counteralign spins on neighbouring Cu d-orbitals as was first suspected by Anderson in 1959 [12]. This antiferromagnetic state (also called Néel ordered phase) is apparent in Figure 13.

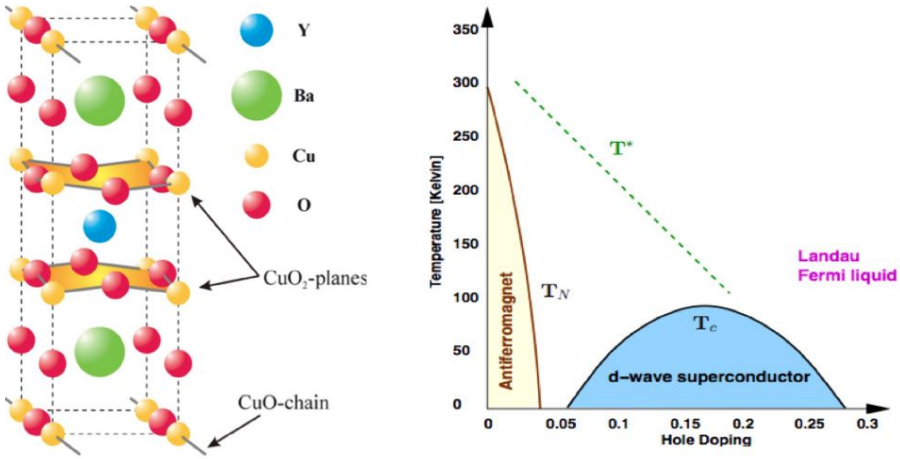

Figure 13: Left: Structure of YBaCuO cuprate, Right: Phase diagram of superconducting cuprates.

5.2 Cuprate superconductivity

In the copper oxide planes of the cuprate superconductors, all $3d$ orbitals are filled except for one vacancy in the $3\,d_{x^2-y^2}$ orbital, so that this orbital becomes half-filled and moreover, a Mott insulator. The conduction channel here is from the $3\,d_{x^2-y^2}$ orbital on one Cu atom, via the oxygen $2\,p_x$ or $2\,p_y$ orbitals, to the $3\,d_{x^2-y^2}$ orbital on the next Cu atom (see Figure 14). Upon hole doping the cuprate, a percentage of the electrons in the $3\,d_{x^2-y^2}$ orbitals make place for a vacancy, making the conduction channel wider. I like Jan Zaanen's explaination of the Mott insulator as "just the incarnation of rush hour traffic in the world of electrons" and of doping the system as "the $\hbar$ version of stop-and-go traffic" [13]. When increasing the hole concentration over about 5%, the system not only gets out of the Mott insulating phase, but also becomes slightly superconducting as you probably noticed in Figure 12. Here I use "slightly", because although some Cooper pairs are formed at ~5% hole doping, it takes a higher doping concentration (~ 15%) to get to a truly superconducting state.

Superconducting behavior in lanthanum barium copper oxide was first discovered by Georg Bednorz and Alex Müller in 1986. The critical temperatures of the cuprate superconductors are notoriously high, which explains the term high $-T_c$ superconductors. In general, opinions on whether we found a proper explanation for this cuprate 3 $d_{x^2-y^2}$ orbital superconductivity are mixed, although Anderson claims to have found the solution years ago. Because the matter is quite complicated, we will only shortly address his Resonant Valence Bond (RVB) theory, which he had developed earlier.

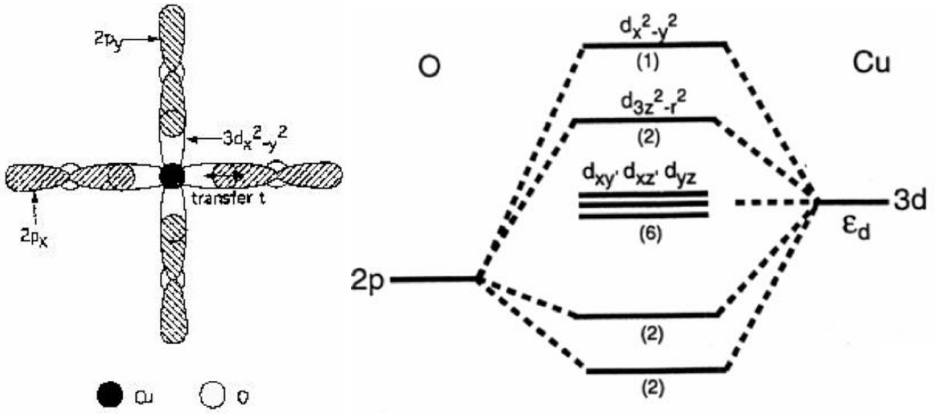

Figure 14: Left: 3 $d_{x^2-y^2}$ orbital with ligand oxygen 2 p_x and 2 p_y orbitals, Right: Energy levels of CuO valence bonds, by Fulde (1991)

RVB theory builds upon the dimerization of the antiferromagnetic Cu lattice into a Valence Bond Solid, or VBS. These "dimers" consist of a spin up and a spin down electron on two nearest neighbour Cu 3 $d_{x^2-y^2}$ orbitals (Figure 15) and are singlets. In Anderson's model, the system is not dimerized in a single way, but in a superposition of all different ways to pair the electrons. This allows for quantum fluctuations in the valence bond configuration and explains the name Resonant Valence Bond theory.

According to RVB theory, addition of holes to the system causes some of the electron pairs that formed a dimer, to become superconducting Cooper pairs. Anderson argues that the pairing between the electrons would not break when hole doping pushes the system through the Mott-Metal transition since breaking up the valence bonded pair costs an energy $\sim J$ [14].

I would like to note that in his papers, Anderson strikes me as very assured of his theories. This is probably due to his status and agressive but sophisticated way of writing, supported by the occasional honest remark of something minor that 'may be uncertain'. But although some evidence for a RVB state has been found in exotic materials, a solid confirmation of RVB being the physical origin for cuprate superconductivity is still missing. The theory seems to remain a - very - educated guess.

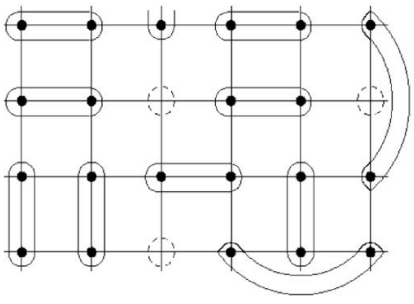

Figure 15: Dimerization of a square lattice of copper atoms

6 Exotic Mott insulator systems

Mott insulating effects occur in a large number of compounds. It should therefore not surprise you that there also exist some Mott insulating materials with additional exotic effects. Think of considerable spin-orbit coupling or topological insulator effects... Furthermore, the artificial Mott insulating systems we developed in the recent years - especially optical traps - allow us to introduce numerous effects to the Mott insulating system and study the consequences. In this section I will, very briefly, discuss some of these exotics.

6.1 Mott insulators with high spin-orbit coupling

Heavy Mott insulating materials may also exhibit considerable spin-orbit coupling. This adds an extra term

$$\mathcal{H}_\lambda = \lambda \sum_i \hat{L}_i \cdot \hat{S}_i. \tag{26}$$

which supports the potential or U term. Consequently, these heavy materials sometimes don't need high Coulomb potentials to become Mott insulators. One may also need to include the spin-orbit interaction in the form of a Rashba Hamiltonian:

$$\mathcal{H}_R = \lambda \sum_{\langle i,j \rangle} \hat{c}_j^\dagger \left(\vec{\sigma} \times \vec{d}_{ij} \right) \hat{c}_i, \tag{27}$$

where d_{ij} is the vector between sites i and j. The Rashba Hamiltonian couples hopping to variations in spin. This introduces interesting effects as finite momentum superfluids with complex phase patterns and may break the Mott insulating state [15].

6.2 Topological Mott insulators

Some materials that show high spin-orbit interactions, may also exhibit topological insulating properties. These are reasonably called Topological Mott Insulators or MIT's. Like most topological insulators, they show nontrivial edge states and are characterized by a nonzero Chern number.

Unlike "conventional" topological insulators, TMI's have gapless edge "spinons". These spinons are chargeless particles with the spin of an electron. These emerge when electrons in a quantum spin liquid (similar to Anderson's RVB state from the previous section) become deconfined, together with a spinless holon that carries the electron charge.

TMI's have been created in 1D optical Mott lattices by, among others, Yoshida et. al. (2014) [16].

6.3 Proximity effects in topological insulator and Mott insulator heterostructures

Like often used with superconducting materials, topological insulators may also affect the electric behaviour of nearby materials. Ueda et. al. (2013) [17] performed a theoretical study on the effect of a topological insulator(TI) - Mott insulator(MI) heterostructure where a thin layer of TI is sandwiched between MI materials. Here the left and right MI materials are modelled as:

$$\mathcal{H}_{\mathrm{MI}} = \mathcal{H}_R + \mathcal{H}_L + \mathcal{H}_V^{\mathrm{RL}} \tag{28}$$

where

$$\mathcal{H}_{R,L} = t \sum_{\langle i,j \rangle, \sigma} \hat{c}_{i,\sigma}^\dagger \, \hat{c}_{j,\sigma} + U \sum_i \hat{n}_{i,\uparrow} \, \hat{n}_{i,\downarrow} \quad \text{and} \quad \mathcal{H}_V^{\mathrm{RL}} = \sum_{\langle i,j \rangle, \sigma} V\big(\hat{c}_{i,\sigma}^\dagger \, \hat{a}_{j,\sigma} + \hat{a}_{i,\sigma}^\dagger \, \hat{c}_{j,\sigma}\big). \tag{29}$$

Here $\mathcal{H}_R$ and $\mathcal{H}_L$ are the single band Hubbard Hamiltonians of the left and right MI materials and $\mathcal{H}_V^{\mathrm{RL}}$ is the hybridization matrix. The operator $\hat{a}_{i,\sigma}^{\dagger}$ creates an electron in the TI region so that the hybridization matrix elements reflect hopping from a MI region onto the TI and back onto a MI region. The TI region is described as

$$\mathcal{H}_{\mathrm{TI}} = \mathcal{H}_{\mathrm{BHZ}} + U_{\mathrm{TI}} \sum_i \hat{n}_{i,\uparrow}\, \hat{n}_{i,\downarrow}, \tag{30}$$

but we will not examine this any further as the Bernevig-Hughes-Zhang Hamiltonian is not within the scope of this report. Ueda et. al. used dynamical mean-field theory (DMFT) to find that the helical edge states of the TI penetrate into the MI to cause a mid-gap band that shows the remains of the helical energy spectrum of the TI. This effect occurs even if the Hubbard gap is very large.

7 Closing Remarks

During my search for literature about the Mott insulator, I stumbled upon quite a high barrier that separates the egg-crate explanations from the more sophisticated quantum mechanical treatments. While the egg-crate model is explainable to the average Joe, reading a paper on Mott insulator systems requires both a decent education in solid state physics and a handful of subject specific experience that is only gained by studying multiple of these papers. With this crude introduction to Mott insulators I hope to make the climb over said barrier easier to take. For me personally, writing this report has given me insight in a branch of solid state physics I was not familiar with and has proven me to be very interesting.

We have seen in chapters 3 and 4 that there are multiple ways to experimentally gain more insight in the physics of Mott insulators and that these physical setups are in strong agreement with the developed mathematical framework of chapter 2. Nevertheless, chapters 5 and 6 have shown us that there are plenty of unresolved discussions about Mott insulator phenomena, that probably will not end anytime soon.

Though certainly underexplored and therefore interesting in their own right, the exotic systems of chapter 6 are not expected to clarify much of our understanding of the Mott metal-insulator transition itself. A definite theory of high-T_c superconductivity however, may very well coincide with a more profound understanding of Mott insulators. This makes both high-T_c superconductivity and the Mott metal-insulator transition interesting fields to study or at least monitor during the upcoming decade.

References

[1] de Boer, J.H. and Verwey E.J.W. (1937). Proc. Phys. Soc. London, Sect. A **49**, 59.

[2] Mott, N.F. and Peierls, R. (1937). Proc. Phys. Soc. London, Sect. A **49**, 72.

[3] Gantmahker, V.F. (2005). Oxford Science Publications.

[4] Hubbard, J. (1963). Proc. R. Soc. London, Ser. A **276**, 238.

[5] Imada, M.; Fujimori, A.; Tokura, T. (1998). Rev. Mod. Phys. Vol **70**, No 4.

[6] van Oosten, D. (2004). PhD Thesis; Quantum gasses in optical lattices; the atomic Mott insulator.

[7] Jördans, R.*;* Strohmaier, N.; Günther, K.; Moritz, H. and Esslinger, T. (2008). Nature Letters Vol. **455**.

[8] Nelson, D.R. and Vinokur, V.M. (1993). Phys. Rev. B., **48**, 17.

[9] Poccia, N.; Baturina, T.I.; Coneri, F.; Molenaar, C.G.; Wang, X.R.; Bianconi, G.; Brinkman, A.; Hilgenkamp, H.; Golubov, A.A. and Vinokur, V.M. (2014). arxiv.org/pdf/**1408.5525**.pdf

[10] Kotliar, G.; Lange, E; Rozenberg, M.J. (2000). Phys. Rev. Letters, **84**, 22.

[11] Spałek, J. (2007). Phys. Rev. B., **48**, 17.

[12] Anderson, P.W. (1959). Phys. Rev. Vol **115**, No 1.

[13] Zaanen, J. (2010). arxiv.org/pdf/**1012.5461v2**.pdf

[14] Anderson, P.W. (1987). Science Vol **235**, p. 1196.

[15] Qian, Y.; Gong, M.; Scarola, V.W. and Zhang, C. (2013). arxiv.org/pdf/**1312.4011**.pdf

[16] Yoshida, T.; Peters, R.; Fujimoto, S. and Kawakami, N. (2014). arxiv.org/pdf/**1405.2147v1**.pdf

[17] Ueda, S.; Kawakami, N.; Sigrist, M. (2014). arxiv.org/pdf/**1303.2781v1**.pdf

Appendix

```
(*----------Script   for   a   simplified   bosonic   Mott   model----------*)

Clear[m, n, t, c, i, k];

m = 10; (*Lattice dim in y-dir*)
width = m*2; (*Lattice dim in x-dir*)
tmax = 20;

(* ---- Generates supply of random (but unique) {x,y} coordinates ---- *)
z = width*m*4;
xini1 = RandomChoice[Range[width], z];
yini1 = RandomChoice[Range[m], z];
randomwell = Table[0*i*k, {i, z}, {k, 2}];

Do[randomwell[[i, 1]] = xini1[[i]], {i, z}];
Do[randomwell[[i, 2]] = yini1[[i]], {i, z}];

Do[
  Do[
    If[randomwell[[i]] == randomwell[[j]], randomwell[[i]] = {0, 0}];
    , {j, i + 1, z}];
  , {i, z}];

pos = Position[randomwell, {0, 0}];
randomwell = Delete[randomwell, pos];
(* ---- End of random generator ---- *)

(*Define some empty variables with right dim*)
sxn = Table[i*0, {i, 100}];
fulltn = Table[i*0, {i, 100}];
hlmvctn = Table[i*0, {i, 100}];

(*Iterates for all defined filling percentages*)
Do[
  n = Floor[width*m*0.01*f];
  Efield = 2;
  echarge = 1;

  (*Makes 100% electron lattice*)
  full = Table[0*i*k, {i, 1, m*width}, {k, 2}];
  c = 0;
  Do[
   Do[full[[i + c, 1]] = i, {i, 1, width}];
   c = width*b;
   , {b, 1, m}];
  c = 0;
  Do[
   Do[full[[i + c, 2]] = b, {i, 1, width}];
   c = width*b;
   , {b, 1, m}];

  (*define some variables*)
  numbofholes = m*width - n;
  exclude = Table[randomwell[[i]], {i, 1, numbofholes}];

  sx = Table[0*i, {i, tmax}];
  sx[[1]] = exclude;

  (*subtract holes from electron lattice for init cond.*)
  fulld = full;
  Do[
   pos = Position[fulld, exclude[[i]]];
   fulld = Delete[fulld, pos];
   , {i, 1, numbofholes}];
```

```
  (*making more empty vars at correct dim*)
  fullt = Table[0*i, {i, tmax}];
  fullt[[1]] = fulld;

  t = 1;
  q = Table[0*i, {i, numbofholes}];
  a = Table[0*i, {i, 2}];
  hlmvct = Table[0*i, {i, tmax}];

  (*iterates over time before tmax*)
  While[t < tmax,
   old = sx[[t]];
   hlmvct2 = 0;

   (*iterate over all hole sites*)
   Do[
    g = old[[i]];

    (*If x coordinate of hole is on left edge, move to right edge*)
    If[g[[1]] < 2, gxn = width, gxn = g[[1]] - 1];
    g[[1]] = gxn;
    (*If position left of hole is electron, move hole one site to left*)
    If[MemberQ[old, g] == True, q[[i]] = old[[i]], And[q[[i]] = g, hlmvct2 = hlmvct2 + 1]];

    , {i, 1, numbofholes}];

   (*write number of moved holes at latest t to global variable*)
   hlmvct[[t + 1]] = hlmvct2;
   (*write new position of holes to global variable*)
   sx[[t + 1]] = q;

   (*subtract holes from full electron lattice*)
   fulld = full;
   Do[
    pos = Position[fulld, q[[k]]];
    fulld = Delete[fulld, pos];
    , {k, 1, numbofholes}];

   (*write new position of electrons to global variable*)
   fullt[[t + 1]] = fulld;

   t = t + 1;
   ];

  (*write all global vars to position for fill fraction f*)
  sxn[[f]] = sx;
  fulltn[[f]] = fullt;
  hlmvctn[[f]] = hlmvct;

  , {f, {25, 50, 75, 90, 95, 100}}];

(*visualisation and interface*)
Manipulate[
 fullt = fulltn[[f]];
 sx = sxn[[f]];
 hlmvct = hlmvctn[[f]];

 Animate[Graphics[{
    {Text["Number of electrons that hopped right: ", {2, -1}]},
    {Text[hlmvct[[t]], {6, -1}]},
    {Red, PointSize -> .01, Point[{fullt[[t]]}]},
    {Blue, PointSize -> .01, Point[{sx[[t]]}]},
    {Black, Line[{{0, 0}, {width + 1, 0}}]},
    {Black, Line[{{0, m + 1}, {width + 1, m + 1}}]},
    {Black, Line[{{0, 0}, {0, m + 1}}]},
    {Black, Line[{{width + 1, 0}, {width + 1, m + 1}}]}
    }, PlotRange -> {{-2, width + 2}, {0 - 2, m + 2}}, ImageSize -> Large], {t, 1, tmax,
1}, AnimationRate -> 1.5]
```